Signals for Specular Andreev Reflection

Qingyun Zhang, Deyi Fu, Baigeng Wang, R. Zhang, and D. Y. Xing

National Laboratory of Solid State Microstructures and Department of Physics, Nanjing University, Nanjing 210093, China

(Received 24 April 2008; published 25 July 2008)

We report a theoretical investigation of the spin-dependent Andreev reflection at the interface of a graphene-based ferromagnet/superconductor junction. It is found that the ferromagnetic exchange interaction in the ferromagnet can suppress Andreev retroreflection but enhance the specular Andreev reflection. There is a transition between the specular Andreev reflection and Andreev retroreflection at which the shot noise vanishes and the Fano factor has a universal value. The present work provides a new method of detecting the specular Andreev reflection, which can be experimentally tested within the present-day technique.

DOI: 10.1103/PhysRevLett.101.047005 PACS numbers: 74.45.+c, 73.23.−b, 74.78.Na

The conventional Andreev reflection process [1–3] at the interface between a normal metal (N) and a superconductor (S) means that an electron in the N impinging on the N/S interface is converted into a hole with a Cooper pair transferred into the superconductor. Since the reflected hole retraces the path of the incident electron, the conventional Andreev reflection is also called retroreflection. Very recently, Beenakker [4] predicted that a graphene-based N/S junction can exhibit both Andreev retroreflection and specular Andreev reflection due to the unique energy band structures of graphene. From the physical point of view, if two electrons involved in the Andreev reflection process come from the same band (conduction band or valence band), this Andreev reflection is the conventional retroreflection. Otherwise, a specular Andreev reflection happens when the two electrons come from conduction and valence bands, respectively. A natural question arises: How can the specular Andreev reflection be experimentally distinguished from the conventional retroreflection?

In this Letter, we study the transport properties of a graphene-based ferromagnet/superconductor (F/S) junction by using the scattering matrix approach. It is found that the Andreev retroreflection and specular reflection are strongly affected by a new energy scale—the exchange energy m of the ferromagnetic graphene. When the Fermi level is out of the $(-m, m)$ window, the Andreev reflection is the conventional Andreev retroreflection, and the zero-bias conductance is suppressed by the exchange interaction. If the Fermi level lies within the $(-m, m)$ window, however, the specular Andreev reflection dominates the conduction, and the zero-bias conductance is enhanced by the exchange interaction. Further study shows that a vanishing shot noise point and a universal Fano factor $F = \frac{18\pi-56}{12-3\pi} \approx 0.213$, corresponding to the closed channel case, characterize a transition between the two kinds of Andreev reflections. The universal Fano factor $F = 0.213$ is independent of the mismatch of the Fermi wavelength between the F and S regions.

The model that we consider is a graphene-based F/S junction. In the ferromagnetic graphene region for $x < 0$, the ferromagnetic correlation may be either extrinsically or intrinsically induced [5]. In the mean-field framework, we use an effective one-electron Hamiltonian with exchange energy m mimicking the ferromagnetic correlation. In the region of $x \geq 0$, the conventional s-wave superconducting state is maintained by putting a superconducting electrode on top of the graphene sheet [6]. The electron and hole excitations in this graphene-based F/S junction can be described by the Dirac–Bogoliubov–de Gennes equation [4,7–9]

$$\begin{pmatrix} H_{a\sigma} - E_F + U(r) & \Delta(r) \\ \Delta^*(r) & E_F - U(r) - H_{a\bar{\sigma}} \end{pmatrix} \psi_a = E\psi_a. \tag{1}$$

Here $\psi_a \equiv (\psi_{Aa\sigma}, \psi_{Ba\sigma}, \psi^*_{A\bar{a}\,\bar{\sigma}}, -\psi^*_{B\bar{a}\,\bar{\sigma}})$ are the four components spinor wave functions, with A and B indicating two inequivalent sites in the hexagonal lattice of graphene. The subscript a denotes two valleys of the band structure K and K', and σ ($\bar{\sigma}$) is the spin index. If $a = K$ (K'), we have $\bar{a} = K'$ (K), and $\bar{\sigma}$ is the spin opposite to σ. E_F is the Fermi energy, and the pair potential $\Delta(r)$ which couples the electron and hole excitations from different valleys is of the form $\Delta_0 \exp(i\phi)\Theta(x)$, with ϕ the superconducting phase and Θ the step function. $H_{a\sigma} = -i\hbar v_F[\sigma_x \partial_x + \mathrm{sgn}(a)\sigma_y \partial_y] - \sigma m\Theta(-x)$ is the two-dimensional Dirac Hamiltonian, with v_F the Fermi velocity of quasiparticles in graphene. $\sigma = +$ $(-)$ stands for spin up (down) and $\mathrm{sgn}(a) = +1$ (-1) for $a = K$ (K'). m is the exchange energy, and σ_x and σ_y are the Pauli matrices acting on two sublattices. Equation (1) can describe both graphene-based ferromagnetic metal with $\Delta_0 = 0$ and graphene-based superconductor with $m = 0$. Note that we have set a single-body potential $U(r) = -U_0\Theta(x)$ in the S region and have assumed $U_0 + E_F \gg \Delta_0$. This condition is the requirement of superconductivity, indicating that the Fermi wavelength in the S is much smaller than the superconducting coherence length [2]. In the numerical calculations below, the single-body potential U_0 always satisfies $U_0 \gg \Delta_0$ unless we specify.

Following the method in Refs. [4,7,8], we can readily solve the Dirac–Bogoliubov–de Gennes equation. The key point is that we must consider two spin-dependent processes due to the splitting of spin bands induced by the exchange interaction. The wave functions in two regions can be written as $\Psi_F = \psi_F^{e+} + r\psi_F^{e-} + r_A\psi_F^{h-}$ and $\Psi_S = t\psi_S^e + t'\psi_S^h$. Here $\psi_F^{e\pm}$ and $\psi_F^{h\pm}$ are the electron and hole wave functions, respectively, in the F region, and ψ_S^e and ψ_S^h are the wave functions of electronlike and holelike quasiparticles, respectively, in the S region. At the boundary, the wave functions must satisfy the continuous condition: $\Psi_F|_{x=0} = \Psi_S|_{x=0}$. A straightforward calculation gives the spin-dependent normal reflection coefficient r_σ and the Andreev reflection coefficient $r_{A\sigma}$ as

$$r_\sigma = \frac{C_\sigma e^{i\alpha_\sigma} - D_\sigma}{C_\sigma e^{-i\alpha_\sigma} + D_\sigma}, \qquad r_{A\sigma} = \frac{2\cos\alpha_\sigma \cos\gamma}{C_\sigma e^{-i\alpha_\sigma} + D_\sigma}, \quad (2)$$

where $C_\sigma = \cos(\gamma - \beta) + i\sin\beta e^{-i\alpha'_\sigma}$ and $D_\sigma = \cos(\gamma + \beta)e^{-i\alpha'_\sigma} + i\sin\beta$, with $\alpha_\sigma = \sin^{-1}[\hbar v_F q/(E + E_F + \sigma m)]$ as the injection angle of electrons and $\alpha'_\sigma = \sin^{-1}[\hbar v_F q/(E - E_F - \bar{\sigma} m)]$ as the Andreev reflection angle of holes. The parameter β is taken to be $\cos^{-1}(|E|/\Delta_0)$ for $|E| \le \Delta_0$ or $-i\cosh^{-1}(|E|/\Delta_0)$ for $|E| > \Delta_0$, and $\gamma = \sin^{-1}[\hbar v_F q/(U_0 + E_F)]$.

Once obtaining these coefficients, we then calculate the charge current through the junction by using the well-known Blonder-Tinkham-Klapwijk formula [10]

$$I = \frac{2e}{h}\sum_\sigma \int_{-\infty}^{+\infty} dE D_\sigma(E) \int [T_A^\sigma (f^- - f^+) + (1 - T^\sigma - T_A^\sigma)(f^- - f)]\cos\alpha_\sigma d\alpha_\sigma. \quad (3)$$

Here the factor 2 comes from the valley degeneracy. $T^\sigma = |r_\sigma|^2$ and $T_A^\sigma = |r_{A\sigma}|^2 \frac{\cos\alpha'_\sigma}{\cos\alpha_\sigma}$ are the probabilities of the normal reflection and Andreev reflection, respectively [11]. The Fermi distribution functions are defined as $f = 1/(e^{\beta E} + 1)$ and $f^\mp \equiv f(E \mp eV)$. $D_\sigma(E) = \frac{|E + (E_F + \sigma m)|w}{\pi\hbar v_F}$ is the number of transverse modes, with w the width of the junction. Equation (3) is one of our main results in this work, which describes the Andreev current and quasiparticle current for the graphene-based F/S junction at the arbitrary temperature and bias. In what follows, we focus on the low-temperature case of the bias smaller than the superconducting energy gap, since we are interested only in the Andreev reflection process.

Figure 1 shows the zero-bias conductance versus exchange interaction m for different E_F. It is found that the conductance is suppressed by increasing m for larger E_F. This behavior has been well understood in the conventional F/S junction. Surprisingly, as E_F decreases, the conductance as a function of m exhibits nonmonotonic behavior. The conductance decreases from $m = 0$ to E_F and $G = 0$ at $m = E_F$ and then goes up. In particular, at $E_F = 0$, the conductance increases linearly from the beginning. In order to get more physics, we divide E_F into two regions $|E_F| \le m$ and $|E_F| > m$ in terms of a new energy scale—exchange energy m. The Andreev reflection processes in the two regions are shown in Figs. 2(a) and 2(b), respectively. If E_F lies within the $(-m, m)$ window, an electron with spin up in the conduction band is reflected as a hole in the spin-down valence band, and so only the specular Andreev reflection contributes to the zero-bias conductance. In contrast, when E_F is out of the $(-m, m)$ window, the two electrons participating in the Andreev reflection process come from the conduction (valence) band, giving rise to the Andreev retroreflection. It then follows that the exchange interaction suppresses the conventional Andreev retroreflection [3] but enhances the specular Andreev reflection. This result provides the first criterion for distinguishing the specular Andreev reflection from the conventional Andreev retroreflection.

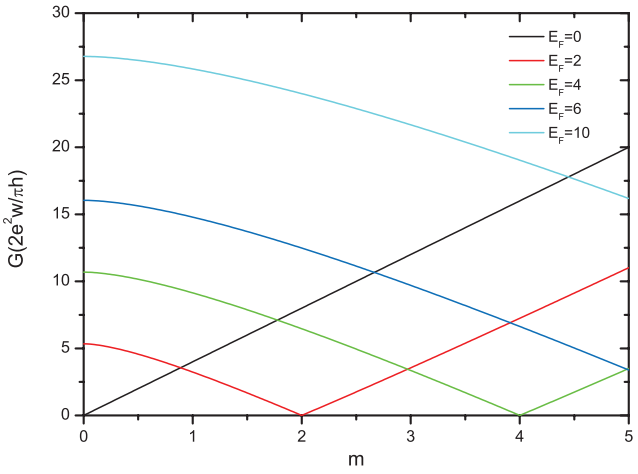

FIG. 1 (color). Zero-bias conductance of the graphene-based F/S junction as a function of exchange energy m for different Fermi energies. Here $U_0 = 1000$ is taken with Δ_0 as the unit of energy (in reality, all of the results remain unchanged on the whole provided that $U_0 > 80$). The series of curves, from left to right, are plotted for $E_F = 0$, 2, 4, 6, and 10.

Apart from the conductance, the shot noise can also provide useful information not available from the dc current alone, since it represents the temporal fluctuation of charge current out of equilibrium caused by the discreteness of charges. Very recently, several works have paid attention to the shot noise spectrum of graphene whose low-energy excitation behaves like the massless Dirac fermions. Theoretically, Tworzydło *et al.* [12] first predicted that the Fano factor reaches a universal maximum $F \sim 1/3$ at zero carrier concentration (the Dirac point). Later, two experimental groups of Danneau *et al.* and DiCarlo *et al.* [13,14] confirmed the theoretical result in both ballistic and disordered graphenes. Here we consider the zero-frequency shot noise for the graphene-based F/S junction, which is generally defined by [15,16] $S = 2\int_{-\infty}^{+\infty} dt \langle[\hat{I}(t) - \langle I\rangle] \times [\hat{I}(0) - \langle I\rangle]\rangle$. In the Andreev re-

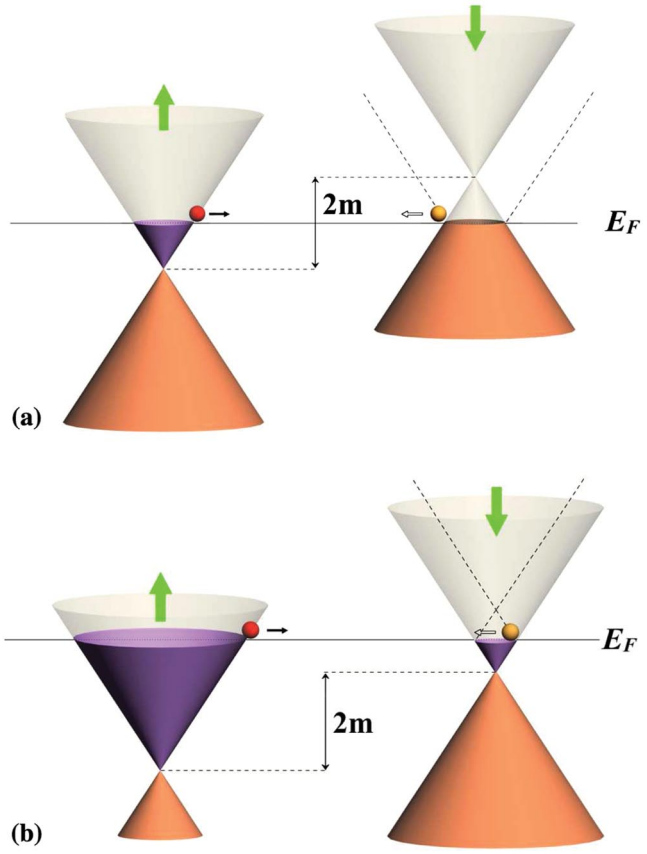

FIG. 2 (color). (a) Specular Andreev reflection process. Horizontal arrows indicate the direction of the velocity, and the dashed lines describe the hole band. (b) Andreev retroreflection process.

flection region, it can be written as

$$S = 16\frac{e^3V}{h}\sum_{\sigma} D_{\sigma}(0)\int T_A^{\sigma}(1 - T_A^{\sigma})\cos\alpha_{\sigma}d\alpha_{\sigma}. \quad (4)$$

Figure 3 shows the shot noise as a function of E_F for different exchange energies $m = 2$ and $m = 4$. First, it is found that there are two zero points of shot noise at $E_F = 0$ and $E_F = m$. At $E_F = 0$, all of the channels are open due to the electron-hole symmetry, and there is nearly perfect Andreev reflection, regardless of a large Fermi wavelength mismatch. At $E_F = m$, the Fermi surface locates just at the Dirac point of the spin-down band, and so all of the channels are closed. Second, the overall shot noise, which is a product of the average shot noise and the number of channels, first increases and then drops to zero for the specular Andreev reflection ($0 < E_F < m$) but increases monotonically with E_F for the Andreev retroreflection ($E_F > m$). This is because the average shot noise of each channel increases with E_F, but the number of channels contributing to the conduction decreases linearly with E_F increased from 0 to m and then increases for $E_F > m$. The vanishing shot noise at $E_F = m$ due to the closed conduction channel is another criterion of the transition between the Andreev retroreflection and specular Andreev reflection.

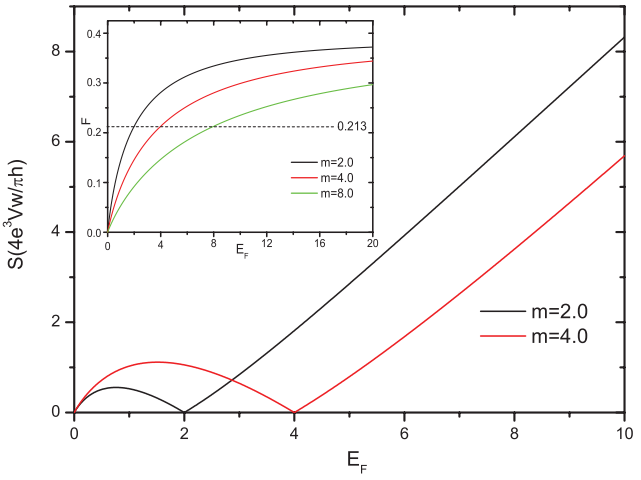

FIG. 3 (color). Shot noise as a function of Fermi energy for fixed exchange energies $m = 2, 4$. Here we have set the temperature to be zero: $eV \ll \Delta_0$. Inset: The Fano factor as a function of Fermi energy for different exchange energies $m = 2, 4, 8$, from top to bottom. Other parameters Δ_0 and U_0 are the same as those in Fig. 1.

Finally, we turn our attention to the Fano factor, which measures the unit of transferred charges. It is defined by $F = S/S_P$, where $S_P = 2eI$ is called the Poisson noise in the absence of statistical correlations between currents. At zero temperature and small bias voltage, the Fano factor has the simplified form

$$F = \frac{\sum_{\sigma} D_{\sigma}(0)\int 2T_A^{\sigma}(1 - T_A^{\sigma})\cos\alpha_{\sigma}d\alpha_{\sigma}}{\sum_{\sigma} D_{\sigma}(0)\int T_A^{\sigma}\cos\alpha_{\sigma}d\alpha_{\sigma}}. \quad (5)$$

The Fano factor variation with E_F is plotted in the inset in Fig. 3. Owing to the large transmission coefficient, it is found that the Fano factor of the graphene-based F/S junction is always sub-Poissonian. In addition, the Fano factor increases monotonically with E_F for $U_0 \gg \Delta_0$, which suggests that the Fano factor in the specular Andreev reflection case ($E_F < m$) is always smaller than that in the Andreev retroreflection case ($E_F > m$). This is because there is no channel mixing in the present model; the change of the Fano factor is caused by the variation of the value distribution of T_A^{σ}. With E_F increased from the specular Andreev reflection to the Andreev retroreflection region, the Andreev reflection probability decreases, so that the integral $\int T_A^{\sigma}\cos\alpha_{\sigma}d\alpha_{\sigma}$ in the denominator of Eq. (5) decreases but $\int 2T_A^{\sigma}(1 - T_A^{\sigma})\cos\alpha_{\sigma}d\alpha_{\sigma}$ in the numerator increases. This fact can account for the monotonic increase of the Fano factor with E_F. Another interesting result is that both the Andreev conductance and shot noise become zero at $E_F = m$, but the Fano factor still has a finite value. This Fano factor at $E_F = m$ defines the boundary between the specular Andreev reflection and

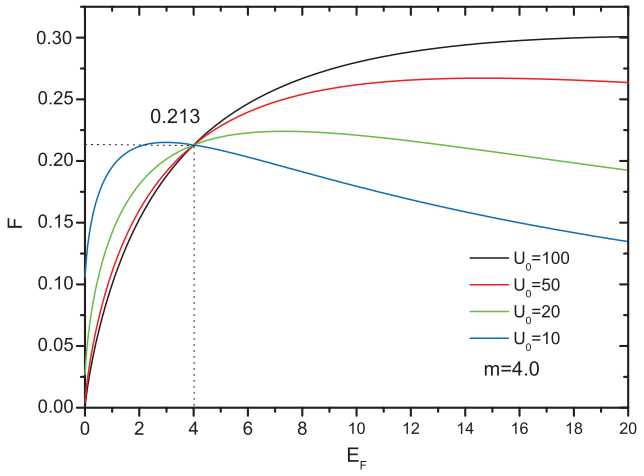

FIG. 4 (color). The Fano factor as a function of the Fermi energy for different single-body potentials $U_0 = 10$, 20, 50, and 100 with $m = 4.0$.

the Andreev retroreflection and can be obtained from the following calculation. At $E_F = m$, the Andreev reflection coefficient is reduced to $T_A^\sigma = 2\cos\alpha'_\sigma/(1 + \cos\alpha'_\sigma)$. In this limit, Fano factor F can be analytically calculated by Eq. (5), yielding a universal value of $(18\pi - 56)/(12 - 3\pi) \approx 0.213$. Note that the universal Fano factor is independent of the single potential U_0, which acts as the source of the Fermi wavelength mismatch between the F and S regions, as shown in Fig. 4. The underlying physics can be understood by the following argument. When the Fermi level locates at the Dirac point of the spin-down band, there is a very large mismatch between the Fermi surface of the spin-down band in the F and that in the S for any finite U_0. Such a large mismatch in the Fermi surface can be regarded as an infinite high barrier at the interface of the F/S junction, which leads to the same Andreev reflection coefficient and the universal Fano factor. At the usual F/S interface, the Andreev reflection decreases with enhancing the interfacial barrier. Owing to the Klein tunneling in the present graphene-based F/S junction, both the Andreev retroreflection and the specular Andreev reflection have no significant dependence on the interfacial barrier. This point has been confirmed by our numerical calculations.

In conclusion, we have presented a theoretical study of the Andreev reflection in the graphene-based F/S junction. It is found that there is a transition between the conventional Andreev retroreflection and the specular Andreev reflection at $E_F = m$. In this transition point, both zero-bias conductance G and shot noise S vanish, and the Fano factor is equal to a universal value of $F \simeq 0.213$. Both G and S exhibit different behavior with m for $E_F > m$ and $E_F < m$, respectively, corresponding to the Andreev retroreflection-dominated and the specular Andreev reflection-dominated regions. These properties can provide new clues for the specular Andreev reflection.

This work was supported by the National Science Foundation of China under Grants No. 10474034 and No. 60421003. B. W. was also supported by the State Key Program for Basic Researches of China under Grants No. 2006CB921803 and No. 2004CB619305.

[1] A. F. Andreev, Sov. Phys. JETP **19**, 1228 (1964).
[2] C. W. J. Beenakker, Rev. Mod. Phys. **69**, 731 (1997).
[3] M. J. M. de Jong and C. W. J. Beenakker, Phys. Rev. Lett. **74**, 1657 (1995).
[4] C. W. J. Beenakker, Phys. Rev. Lett. **97**, 067007 (2006).
[5] Takehito Yokoyama, Phys. Rev. B **77**, 073413 (2008).
[6] H. B. Heersche *et al.*, Nature (London) **446**, 56 (2007).
[7] S. Bhattacharjee and K. Sengupta, Phys. Rev. Lett. **97**, 217001 (2006).
[8] S. Bhattacharjee, M. Maiti, and K. Sengupta, Phys. Rev. B **76**, 184514 (2007).
[9] J. Linder and A. Sudbø, Phys. Rev. Lett. **99**, 147001 (2007).
[10] G. E. Blonder, M. Tinkham, and T. M. Klapwijk, Phys. Rev. B **25**, 4515 (1982).
[11] Although the Andreev reflection coefficient T_A^σ depends on the spin index, the charge current due to the Andreev reflection process is independent of the spin since there is no spin-flip mechanism in our model. Therefore, we need to take into account only the minority spin-down modes.
[12] J. Tworzydło, B. Trauzettel, M. Titov, A. Rycerz, and C. W. J. Beenakker, Phys. Rev. Lett. **96**, 246802 (2006).
[13] R. Danneau *et al.*, Phys. Rev. Lett. **100**, 196802 (2008).
[14] L. DiCarlo, J. R. Williams, Yiming Zhang, D. T. McClure, and C. M. Marcus, Phys. Rev. Lett. **100**, 156801 (2008).
[15] Ya. M. Blanter and M. Büttiker, Phys. Rep. **336**, 1 (2000).
[16] M. J. M. de Jong and C. W. J. Beenakker, Phys. Rev. B **49**, 16070 (1994).